

On possible simplifications in the theoretical description of gas phase atomic cluster dissociation

Massimo Mella^{a)}

School of Chemistry, Cardiff University, Main Building, Park Place, Cardiff CF10 3AT, United Kingdom

(Received 14 October 2008; accepted 15 January 2009; published online 26 February 2009)

In this work, we investigate the possibility of describing gas phase atomic cluster dissociation by means of variational transition state theory (vTST) in the microcanonical ensemble. A particular emphasis is placed on benchmarking the accuracy of vTST in predicting the dissociation rate and kinetic energy release of a fragmentation event as a function of the cluster size and internal energy. The results for three Lennard-Jones clusters (LJ_n , $n=8, 14, 19$) indicate that variational transition state theory is capable of providing results of accuracy comparable to molecular dynamics simulations at a reduced computational cost. Possible simplifications of the master equation formalism used to model a dissociation cascade are also suggested starting from molecular dynamics results. In particular, it is found that the dissociation rate is only weakly dependent on the cluster total angular momentum J for the three cluster sizes considered. This would allow one to partially neglect the J -dependency of the kinetic coefficients, leading to a substantial decrease in the computational effort needed for the complete description of the cascade process. The impact of this investigation on the modeling of the nucleation process is discussed. © 2009 American Institute of Physics. [DOI: 10.1063/1.3078449]

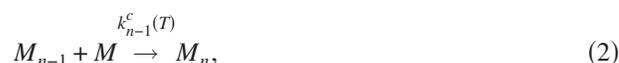
I. INTRODUCTION

The nucleation of a new phase is of fundamental interest in several fields of science, spanning a range including the study of atmospheric phenomena, the possible application to building nanostructures via chemical vapor deposition and the formation of critical germs during crystallization. Even though the thermodynamics of the process seems to have a robust conceptual basis, the phenomenon appears less clear at the molecular level. In fact, the relevant time scales involved in the process of phase formation are still under intense investigation.

In this field, the condensation of a liquid phase starting from a homogeneous supersaturated vapor has received considerable attention from the theoretical chemical physics community during the past few years, perhaps because it might be considered as a simple (but not trivial) representative case of this family of processes. As a consequence, the past decade has witnessed a surge of contributions devoted to improving the understanding of the process time scales, with many studies focusing on the large scale calculation of nucleation rates by means of molecular dynamics (MD),¹⁻⁴ on the benchmark of currently available theories (e.g., classical nucleation theory, extended liquid drop model-dynamical nucleation theory, and other semiphenomenological models),^{1,2,5} and on the calculation of the work necessary to build a cluster from the supersaturated vapor.^{6,7}

Despite these efforts, the routine application of computational approaches to the calculation of nucleation rates for experimentally relevant systems still appears as a distant goal, the exception being perhaps the prediction of the criti-

cal cluster size that can be done by means of thermodynamic integration.⁶ As far as MD simulations are concerned, the main reason for the currently limited applicability is the necessity of simulating large systems with a high degree of supersaturation to witness a condensation event within a reasonable time span. It is therefore in this context that the framework provided by dynamical nucleation theory (DNT), introduced by Schenter *et al.*,⁸ represents an appealing possibility to tackle the same task. In doing so, DNT follows closely the ideas provided by the Szilard model and deals only with two events, namely, the dissociation and condensation of single particles from and to a cluster at constant temperature T



where $k_n^d(T)$ and $k_{n-1}^c(T)$ are the dissociation and condensation rates, respectively. If this was known for the relevant cluster sizes, the time evolution of a nucleating vapor at constant temperature could be predicted using a set of coupled kinetic equations describing $N(n, T)$, the time dependent M_n cluster population. In the case of single monomer evaporation/condensation, this set reads

$$\begin{aligned} \frac{dN(n, T)}{dt} = & k_{n-1}^c(T)N(1, T)N(n-1, T) + k_{n+1}^d(T)N(n+1, T) \\ & - k_n^d(T)N(n, T) - k_n^c(T)N(1, T)N(n, T), \end{aligned} \quad (3)$$

where we have explicitly indicated the dependency on the temperature T of the system and deviated from the usual convention of using the dissociation (α) and condensation

^{a)}Electronic mail: mellam@cf.ac.uk.

(β) coefficients in order to be consistent with the standard chemical kinetics notation. A more general framework than Eq. (3) would be represented by the master equations (MEs) approach,⁹ which would be better suited to follow the time dependent evolution of $N(n, T)$ in more complex cases (e.g., when the single moiety dissociation-association process constraint is lifted⁹), or whenever additional variables are required to describe the system. Starting from Eq. (3), DNT focuses mainly on computing the dissociation rate $k_n^d(T)$ of the n molecule cluster M_n by means of canonical variational transition state theory (vTST). The equilibrium cluster populations $N(n, T)$ (or the free energy difference $\Delta F_{n,n-1} = F_n - F_{n-1}$) and detailed balance are then used to estimate the rate $k_{n-1}^c(T)$ for the inverse condensation process.

In term of its emphasis, DNT differs substantially from other methods that compute k_{n-1}^c by means of simple collision theory arguments and successively estimate k_n^d using the former quantity and the relevant equilibrium constant (for instance, see Ref. 10, and references therein). Unfortunately, methods relying on collision theory are forced to assume a radius r_n for M_n in order to estimate the monomer-cluster cross section in a simple and computationally inexpensive way. Clearly, this introduces a degree of arbitrariness that is not present in DNT, where r_n is instead derived directly from vTST arguments as the location r_n^\ddagger of the spherical separatrix that minimizes the reactive flux. This theoretical advantage, however, is obtained at the price of an increased computational cost (i.e., the one required to estimate k_n^d), a fact perhaps suggesting the need for the development of efficient simulation methods to tackle the task of computing cluster dissociation rates. As a support for this idea, we mention the fruitful attempt made by Crosby *et al.*¹¹ to speed up the calculation of k_n^d within the DNT framework.

In considering the usage of Eq. (3) to describe the system time evolution, it is easy to realize that both k_n^d and k_{n-1}^c could, in principle, be exactly computed using molecular dynamics^{12,13} (MD) without employing statistical theories. The latter, however, provides a computational advantage with respect to MD, which becomes inefficient in computing k_n^d for low temperature (T) or energy (E) clusters. Notice that the choice of the ensemble (i.e., constant T or E), first, depends on the specific details of the process one wishes to simulate and, second, it has an impact on the computational effort needed to study the process as will be discussed in the following. As to the former issue, the use of a constant T ensemble would be justified only for nucleating systems where a sufficiently high number of monomer-cluster collisions take place between two subsequent condensation/dissociation steps, a situation that appears likely only in presence of a sufficiently high bath gas pressure. Besides, both Harris and Ford¹⁴ and Barrett¹⁰ provided computational evidence suggesting that microcanonical MD simulations should be used to describe dissociation events due to a time dependent behavior of the canonical rate constant $k_n^d(T)$ related to the strategy employed to maintain T constant. In the case of zero/low bath gas pressure, of relevance also for constant energy cross beam scattering experiments, the microcanonical ensemble (henceforth indicated either as μ or NVE) appears therefore better suited for the description of

condensation/dissociation events thanks to the fact that E is a constant of motion, a fact suggesting one should focus on the calculation of microcanonical rates [$k_n^d(E)$ and $k_{n-1}^c(E)$]. Following the time evolution of $N(n, E)$ instead of $N(n, T)$, however, increases the computational cost required to predict the nucleation rate due to the necessity of tracking the time evolution of both E and n .

To complicate the matter further, the angular momentum (J -) resolved microcanonical ensemble (indicated as μJ or $JNVE$) should be used instead of NVE in gas phase to account for the constant of motion nature of J . In this case, however, the problem with the scarce efficiency of MD in computing dissociation rates would be exacerbated due to the necessity of integrating the equations of motion for several values of J , a task required not only to obtain the J -dependent behavior of $k_n^d(E, J)$ and $k_{n-1}^c(E, J)$ but also to predict more detailed state-to-state rates such as $k_n^d(E \rightarrow E', J \rightarrow J')$. Here, E' and J' are the internal energy and total angular momentum of the product cluster M_{n-1} , while $k_n^d(E, J)$ and $k_{n-1}^c(E, J)$ are the dissociation and association rates for clusters with total energy E and angular momentum J .

As a consequence of this brief discussion, one should quickly realize the necessity of finding a computationally convenient approach to estimating k_n^d and k_{n-1}^c , for the hope of developing a μ - or μJ -ensemble based numerical scheme able to predict the time dependent behavior of a nucleating system to remain alive. Whereas estimating k_{n-1}^c is expected to be reasonably straightforward and computationally inexpensive thanks to the absence of high energy barriers between impinging monomer and clusters, computing $k_n^d(E)$ should be more expensive than obtaining $k_n^d(T)$. Thus, a statistical theory may, again, represent a practical way of avoiding the high computational cost of long MD simulations, provided that it is shown capable of accurately approximating $k_n^d(E)$. An appropriate statistical theory should also provide an accurate estimate for other quantities such as the kinetic energy release (KER) ($E_{tr} = E_t + E_r$) distribution,¹⁵ i.e., the probability of finding the systems after a dissociation event with the amount of energy E_{tr} injected into relative translational energy E_t of the two fragments and the rotational energy E_r of the remaining cluster. As it should become apparent from the discussion in Sec. II, the KER is a key ingredient needed for setting up the MEs.

Results suggesting the possibility of predicting both k_n^d and the KER distribution for a dissociation event by means of statistical theories have been already presented in the past. For instance, phase space theory^{16,17} (PST) has been previously used to estimate k_n^d for relatively small rare gas¹³ and aluminum¹⁸ clusters and found to perform well. Similarly, Schenter *et al.*¹⁹ provided evidence that their version of canonical vTST, developed to tackle the calculation of $k_n^d(T)$ for molecular clusters, is in agreement with MD results to within a factor of 2. More recently, Calvo and Parneix (Ref. 15, and references therein) investigated the possibility of computing both the KER distribution (i.e., the probability of E_{tr} assuming a specific value ϵ) and the probability of the cluster fragment to have a total angular momentum J' by means of PST, obtaining results that strongly suggested this

theory to be capable of accurately predicting both quantities. Estimating the reaction rate, however, was indicated as a more demanding task due to the necessity of computing accurately the cluster density of states $\Omega(E)$,²⁰ an issue previously discussed in Refs. 13 and 18. To circumvent the latter, Calvo and Parneix²⁰ resorted to calibrating PST dissociation rates against high energy MD simulations, a pragmatic approach that allowed them to apply PST to a sequence of cluster decays.

Apart from the computational difficulties inherent in obtaining $\Omega(E)$, another complication is present in the use of PST for the calculation of $k_n^d(E)$ for a range of cluster sizes, namely, the definition of the asymptotic potential $V_{\text{eff}}(r)$ describing the region of the loose transition state due to relative orbital motion of the two dissociating fragments. In a previous application of the theory, Peshlherbe and Hase¹⁸ resorted to fitting the long range interaction between Al_{n-1} and Al ($n=6, 13$) with the analytical form $-C/r^6$, whereas canonical Metropolis Monte Carlo (MMC) simulations were used to compute the average potential experienced by the detaching fragment in Refs. 13 and 20. In the latter case, the simulation temperature was chosen matching MD and PST results²⁰ despite the fact that $V_{\text{eff}}(r)$ should, in principle, be E -dependent and determined using microcanonical simulations.

Although practical, neither the calibration with MD simulations nor the choice of using a single $V_{\text{eff}}(r)$ for all energies are, in principle, mandatory as they could be circumvented using a different statistical theory merging the appropriate sampling of the reactant configuration space with the accurate determination of key observables, e.g., k_n^d 's and KER distributions. One of the aims of this work is therefore to investigate the accuracy of generalized microcanonical vTST in predicting the latter quantities. Given the four-index dependency of $k_n^d(E \rightarrow E', J \rightarrow J')$, we believe it would also be useful to investigate its sensitivity with respect to the constants of motion E , E' , J , and J' . Quantitative information on this may allow one to devise possible simplification of the MEs, hopefully reducing the number of numerical simulations required to predict vapor condensation or a cluster dissociation cascade. Such an investigation is therefore the second goal of this work.

The outline of this manuscript is the following. In Sec. II, we briefly introduce the theoretical approach used in this work. Section III begins by describing a numerical investigation of the J dependency of $k_n^d(E)$ carried out with MD simulations, its results providing additional evidence for the weak J -sensitivity of this quantity for atomic clusters. With this observation in mind, MD and TST estimates for $k_n^d(E)$ are successively presented for three different Lennard-Jones (LJ) clusters as a benchmark for the accuracy of microcanonical vTST (μ -vTST). Finally, a generalized μ -vTST based approach is proposed to compute the KER distribution with the same statistical simulations used to estimate $k_n^d(E)$. Section IV presents our conclusions and outlook for future applications.

II. THEORY AND SIMULATION METHODS

In this work, we aim toward the development of a TST-based approach for the description of cluster dissociation.

Generally speaking, we wish to build on the evidence that PST provides an accurate alternative to MD and that it is equivalent to more standard vTST in the case of a loose transition state.²¹ In this respect, we begin by considering the use of the TST equation for the classical statistical rate of a dissociation process at constant energy E

$$k_{\text{stat}}^d(E) = \frac{\int_{S^*} \delta[\mathcal{H}(\mathbf{p}, \mathbf{q}) - E] v_{\perp} dS^*}{\int_V \delta[\mathcal{H}(\mathbf{p}, \mathbf{q}) - E] d\Gamma}. \quad (4)$$

Here, S^* is the hypersurface in phase space separating the reactant from the product and v_{\perp} is the velocity perpendicular to this surface and pointing in the direction of the products. The integral at the numerator is carried out over the transition surface (state) S^* , whereas the one at the denominator is computed over the reactant phase space V enclosed by S^* . Often the dependence of S^* on the momenta \mathbf{p} is neglected and only the coordinates \mathbf{q} are used for its definition.

In the case of a simple dissociation process, Eq. (4) can be rewritten as

$$k_{\text{stat}}^d(E) = \frac{1}{2} \frac{\int_V \delta[\mathcal{H}(\mathbf{p}, \mathbf{q}) - E] \delta(r_{\text{IRC}} - r_C) |\dot{r}_{\text{IRC}}| d\Gamma}{\int_V \delta[\mathcal{H}(\mathbf{p}, \mathbf{q}) - E] d\Gamma}, \quad (5)$$

where the distance between the dissociating moiety and the center of mass of the remaining cluster is used as intrinsic reaction coordinate (r_{IRC}), r_C is the critical distance for r_{IRC} (i.e., the location of a spherical S^*), and \dot{r}_{IRC} is the relative velocity of the two dissociating fragments along r_{IRC} . According to the usual vTST prescriptions, r_C must be chosen such that $k_{\text{stat}}^d(E)$ is minimum. Notice that our choice of reaction coordinate is expected to be adequate at low-medium energies, i.e., when the remaining cluster, although fluxional, is still fairly compact. At higher energies, the presence of wide excursions of the surface particles may induce the disappearance of the minimum in $k_{\text{stat}}^d(E)$ as a function of r_C , preventing one from obtaining a theoretically sound estimate for the dissociation rate constant. This difficulty may, however, be cured with a different choice for r_{IRC} .

Assuming $\mathcal{H}(\mathbf{p}, \mathbf{q}) = 1/2 \sum_{i=1}^n \mathbf{p}_i^2/m_i + \mathcal{V}(\mathbf{q})$, the kinetic energy of the system is diagonal in Cartesian coordinates and the integrals in Eq. (5) can be separated obtaining²²

$$k_{\text{stat}}^d(E) = \frac{\int_V [E - \mathcal{V}(\mathbf{q})]^{(3n-5)/2} \delta(r_{\text{IRC}} - r_C) \langle |\dot{r}_{\text{IRC}}| \rangle_K d\mathbf{q}}{\int_V [E - \mathcal{V}(\mathbf{q})]^{(3n-5)/2} d\mathbf{q}}, \quad (6)$$

where $\mathcal{V}(\mathbf{q})$ is the potential energy surface of the system, n is the number of atoms and $\langle |\dot{r}_{\text{IRC}}| \rangle_K$ is the microcanonical ensemble average of the relative velocity of the reactant (R) through the critical surface in the direction of the product (P) for a value of the internal (vibrational plus rotational) kinetic energy equal to $E - \mathcal{V}(\mathbf{q})$. Notice that $[E - \mathcal{V}(\mathbf{q})]^{(3n-5)/2}$ is the appropriate configuration weight for an isolated molecule composed by n atoms as obtained by factorizing out the contribution due to the center of mass motion in the way suggested by Schranz *et al.*²³ An alternative form for Eq. (6) is obtained by using the Heaviside function $H_{>}(\dot{r}_{\text{IRC}})$ selecting velocities directed from R to P and by rewriting the integral ratio as a product of two ratios

$$k_{\text{stat}}^d(E) = \frac{\int_V [E - \mathcal{V}(\mathbf{q})]^{(3n-5)/2} \delta(r_{\text{IRC}} - r_C) \langle H_{>}(\dot{r}_{\text{IRC}}) \dot{r}_{\text{IRC}}(\mathbf{q}) \rangle_K d\mathbf{q} \int_V [E - \mathcal{V}(\mathbf{q})]^{(3n-5)/2} \delta(r_{\text{IRC}} - r_C) d\mathbf{q}}{\int_V [E - \mathcal{V}(\mathbf{q})]^{(3n-5)/2} \delta(r_{\text{IRC}} - r_C) d\mathbf{q}}. \quad (7)$$

In this form, it is made apparent that the calculation of $k_{\text{stat}}^d(E)$ could, in principle, be separated in two (or more) parts with different interpretations. In fact, the first ratio represents the expectation value of $\dot{r}_{\text{IRC}} H_{>}(\dot{r}_{\text{IRC}})$ when the system is constrained to have the dissociating moiety at the critical distance r_C (henceforth dubbed as μ -TS ensemble). The second ratio, instead, is the probability of finding the system at the critical distance.

Notwithstanding the fact that $k_{\text{stat}}^d(E)$ could be estimated directly using Eq. (6) (see Ref. 24 for its original description and Ref. 25 for an alternative implementation), the definition of the μ -TS ensemble introduced in Eq. (7) provides one with conceptual and computational advantages. As for the computational side, the probability of finding the system on the separatrix can be efficiently computed by employing microcanonical²⁵ umbrella sampling²⁶ (US) in conjunction with a new estimator for the Dirac delta recently developed by us.²⁷ From the theoretical view point, instead, the advantage comes from the possibility of thinking about the first integral ratio in Eq. (7) as a specific example [i.e., for $\dot{r}_{\text{IRC}} H_{>}(\dot{r}_{\text{IRC}})$] of an expectation value calculation over the μ -TS ensemble (for instance, see Ref. 28, where a similar factorization was previously exploited to correct for the lack of dynamical effects in TST).

From this brief discussion, it should be apparent that substituting \dot{r}_{IRC} with a different dynamical observable would, in principle, give access to the phase space average of the latter when the system is constrained to lie on the separatrix while having $H_{>}(\dot{r}_{\text{IRC}}) = 1$. Thus, the computational machinery developed for $k_{\text{stat}}^d(E)$ may, for instance, lend itself to the calculation of $P_{tr}(E, \epsilon)$, the probability distribution function of finding E_{tr} in the range $[\epsilon, \epsilon + d\epsilon]$ when the reac-

tant has a total internal energy E . This may be possible provided that the relevant dynamical observable E_{tr} can be written, at least, as an implicit function of the system position \mathbf{q} . A similar statement can be made for $P_t(E, \epsilon)$ when only the distribution of E_t is of interest. Needless to say, the importance of $P_{tr}(E, \epsilon)$ and $P_t(E, \epsilon)$ stems from the necessity of defining the internal energy E' of the fragment cluster after a dissociation event to predict the rate of, e.g., a second monomer ejection, and it is therefore of prime interest in the description of multiple cluster decays as thoroughly discussed in Ref. 20.

To derive a mathematical definition for $P_{tr}(E, \epsilon)$ fitting the framework provided by Eq. (7), we start by noticing that it could be approximated by the fractional number of times a system distributed according to the μ -TS ensemble and with $H_{>}(\dot{r}_{\text{IRC}}) = 1$ is found having E_{tr} in the narrow but finite interval $[\epsilon_{tr}, \epsilon_{tr} + \delta\epsilon_{tr}]$. Within this approximation, it is implicitly assumed that no energy exchange takes place between the two dissociating moieties after an event has been dubbed as reactive. Given a specific geometrical configuration \mathbf{q} of the molecules in the system, the instantaneous amount of kinetic energy \mathcal{K} available to the latter is given by $\mathcal{K} = E - \mathcal{V}(\mathbf{q})$, a part of which would be distributed into E_{tr} . If \mathcal{K} is statistically distributed among degrees of freedom, the relative number of times E_{tr} falls within $[\epsilon_{tr}, \epsilon_{tr} + \delta\epsilon_{tr}]$ is simply given by $\langle H_{>}(\dot{r}_{\text{IRC}}) \Delta(\epsilon) \rangle_K$, where $\Delta(\epsilon)$ is a normalized rectangular distribution with nonzero values only in the interval of interest. Taking the limit $\delta\epsilon_{tr} \rightarrow 0$ and integrating over all available configuration space with the proper microcanonical weighting [i.e., $[E - \mathcal{V}(\mathbf{q})]^{(3n-5)/2}$ (Ref. 24)], one arrives at

$$P_{tr}^{\text{TS}}(E, \epsilon_{tr}) d\epsilon_{tr} = \frac{\int_V [E - \mathcal{V}(\mathbf{q})]^{(3n-5)/2} \delta(r_{\text{IRC}} - r_C) \langle H_{>}(\dot{r}_{\text{IRC}}) \delta[E_{tr}(\mathbf{q}) - \epsilon_{tr}] \rangle_K d\mathbf{q}}{\int_V [E - \mathcal{V}(\mathbf{q})]^{(3n-5)/2} \delta(r_{\text{IRC}} - r_C) d\mathbf{q}} d\epsilon_{tr}. \quad (8)$$

Here, $E_{tr}(\mathbf{q})$ explicitly indicates the dependency of E_{tr} on the atomic coordinates and $\delta[E_{tr}(\mathbf{q}) - \epsilon_{tr}]$ is used to count the number of occurrences for a specific ϵ_{tr} . In practice, Eq. (8) suggests to use a constrained simulation with r_C chosen according to the variational TST principle and to estimate $P_{tr}^{\text{TS}}(E, \epsilon_{tr})$ by counting the number of times E_{tr} falls in the small range between ϵ_{tr} and $\epsilon_{tr} + \delta\epsilon_{tr}$.

While employing Eq. (8) to obtain $P_{tr}^{\text{TS}}(E, \epsilon_{tr})$, one faces an additional difficulty related to the lack of an analytical form for $E_{tr}(\mathbf{q})$. A possible way to circumvent this issue is to tackle the calculation of $\langle H_{>}(\dot{r}_{\text{IRC}}) \delta[E_{tr}(\mathbf{q}) - \epsilon_{tr}] \rangle_K$ numeri-

cally, i.e., by sampling the particle momenta with the appropriate distribution and subject to the constraint $\mathcal{K} = E - \mathcal{V}(\mathbf{q})$ as suggested in Ref. 29. Practically speaking, the randomly sampled momenta are first used to test if \dot{r}_{IRC} is correctly oriented, and subsequently employed to obtain $E_{tr}(\mathbf{q})$. In the latter, the E_r component in the fragment cluster can be computed using its total angular momentum and the instantaneous position of its constituent atoms to define the inertia tensor, whereas E_t is easily obtained from the relative velocity of the two dissociating fragments. Notice that the numerical scheme just discussed implicitly contains the effect of the

J -dependent dissociation potential, it does not consider the cluster as a spherical object, it assumes a vanishingly small residual interaction between the dissociating moiety and the remaining aggregate, and it is a straightforward adaptation of the approach used to estimate the E_r component for a dissociated MD trajectory.

III. RESULTS AND DISCUSSION

A. Behavior of $k_n^d(E, J)$ as a function of the total angular momentum J

As mentioned in Sec. I, the task of modeling vapor nucleation using a set of MEs would be substantially simplified if one was allowed to neglect the dependence on the system angular momentum J . It therefore appears important to explore whether the weak sensitivity of $k_n^d(E, J)$ on J , the angular momentum of the parent cluster, suggested for LJ₁₂₋₁₄ (Ref. 13) and Al₆ (Ref. 18) is more generally valid. We reiterate that the reason for this investigation is the fact that predicting dissociation rates in gas phase would, in principle, force one to work within the framework provided by the μJ -ensemble. Thus, a (partial) justification is needed for the usage of the simpler μ ensemble when there is no interest in computing the evolution of the total angular momentum or of any related observables during the process modeled (e.g., an evaporation cascade).

In order to test such a hypothesis on slightly more general grounds than provided by Refs. 13 and 18 the dissociation rates of three different LJ _{n} clusters ($n=8, 14$ and 19) were computed as a function of both E and J using MD trajectories. These three values of n were selected in order to explore archetypal structural changes between reactants and products.¹⁵ In particular, $n=8$ presents substantial structural differences from its product, the latter being a high symmetry (D_{5h}) oblate rotor that is expected to be capable of isomerizing in the range of energies amenable to MD simulations.¹⁵ $n=14$ was instead chosen for its low evaporation energy due to its capped icosahedral structure and for the fact that it produces a spherical species, whereas $n=19$ was selected to explore the effect of breaking the compact structure of a nonspherical magic number cluster. Figure 1 shows the minimum energy structures for the clusters relevant to this study.

For all systems, the details of the simulations employed to compute the reaction rates are the following. Atoms were assumed to interact by means of a pairwise LJ potential written as $V(r)=4\epsilon[(\sigma/r)^{12}-(\sigma/r)^6]$, with the parameters ($\epsilon=3.7935\times 10^{-4}$ hartree and $\sigma=6.4354$ bohr) being chosen to represent the Ar–Ar interaction. A mass of 73 350.6 times the electron mass was used for the Ar atoms. For each cluster, an initial equilibration stage was conducted at the appropriate total energy E by means of a MMC simulation in the microcanonical ensemble;²⁴ each of the atoms in the cluster was also constrained to have its distance from the center of mass of the remaining ones shorter than 4σ . Trajectories were started from statistically independent samples extracted from the MMC simulations; 10,000–25 000 total trajectories per (n, E, J) triplet were employed to estimate dissociation rates. In the triplet, E is the total energy of a cluster and includes the contribution from the potential energy, the rota-

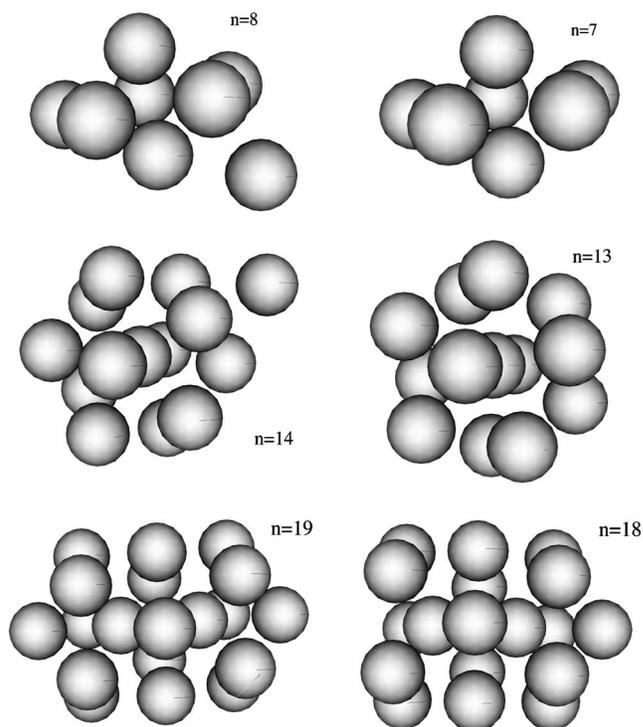


FIG. 1. Minimum energy structure for the reactant (left, LJ_{8,14,19}) and product (right LJ_{7,13,18}) clusters. The energy of the global minimum for $n=7, 8, 13, 14, 18,$ and 19 are, respectively, $-0.006\ 261\ 317,$ $-0.007\ 519\ 282,$ $-0.016\ 815\ 372,$ $-0.018\ 150\ 06,$ $-0.025\ 238\ 516,$ and $-0.027\ 563\ 488$ hartree.

tional kinetic energy, and the vibrational kinetic energy but not from the center of mass motion. Trajectories were integrated using the leap frog algorithm and a time step of 200 a.u. (roughly 5 fs) up to a maximum of 120 ps. The total energy was conserved better than 10 ppm in all cases. Initial velocities for all particles were chosen according to the stochastic procedure suggested in Ref. 29. The total angular momentum was sampled employing a simple rejection procedure with a sampling window of six atomic units of angular momentum \hbar centered around the chosen J value. To select physically sensible values for the latter quantity, short preliminary MMC simulations were carried out on each LJ _{n} at the chosen E . During the MMC sampling, initial velocities for the particles were chosen as indicated above (see Ref. 29) and used to produce the probability distribution $p(J)$ for J at the specific E . In general, such distributions are well approximated by the canonical-like density $p(J)\sim J^2\exp[-\alpha J^2]$. The upper limit of the range of J explored in the MD simulations was chosen as the value $J_{\text{upper}}>J_{\text{max}}$ for which $p(J_{\text{upper}})/p(J_{\text{max}})\sim 0.2$, with J_{max} being the position of the maximum in $p(J)$; with this choice, $\int_0^{J_{\text{upper}}}p(|J|)d|J|/\int_0^\infty p(|J|)d|J|>0.85$ for every E . As final comment, we notice that an explicit dependency on J of the cluster structure and dynamics is introduced only at the beginning of the MD trajectory. However, the initial trajectory configurations partially accounts for some angular momentum effect due to the microcanonical sampling. Also, a substantial re-equilibration of the clusters is allowed by their reasonably long lifetime (see below).

During a trajectory evolution, a particle was considered

dissociated when its distance from the center of mass of the remaining cluster was larger than 4σ , a region for which the interaction potential between the two dissociating fragments was found negligible. The MD rate constants were estimated assuming a first order kinetic law and fitting the long time behavior of $\ln[(N_0 - N_t)/N_0]$ with a straight line. Here, N_0 is the total number of trajectories and N_t is the number of trajectories dissociated at time t . This approach differs somewhat from the procedure used by Weerasinghe and Amar,¹³ who used the last negative minimum of the radial momentum for the dissociating atom to define the dissociation time. It also introduces some arbitrariness in the results, which are independent of the separatrix location only when the latter is placed in a region where the interaction potential has completely died off. Preliminary test runs, however, provided evidence that the rate constants are fairly insensitive to the critical dissociation distance, provided the residual potential is small. Thus, 4σ was found to represent an adequate compromise between accuracy and computational cost for all values of n , E , and J . To test for the suitability of the first order kinetic law, trajectories have been also analyzed plotting lifetime distributions. Generally speaking, lifetimes were found to follow the single exponential distribution predicted by the Rice-Ramsperger-Kassel-Marcus (RRKM) theory³⁰ within the statistical precision of our simulations, the only exception being represented by clusters with high internal energy. Even in these cases, however, only minor deviations were noticed as will be discussed in the following.

Figure 2 (panel a) shows the behavior of $k_n^d(E, J)$ as a function of n , E , and J obtained using MD simulations. Panel b in Fig. 2 provides a graphical representation for the probability distribution function $p(|J|)$ of J at the energies employed in the MD simulations. The values of energy used to investigate the J -dependency of $k_n^d(E, J)$ (Fig. 2) were chosen in order to explore situations of medium and high energy content for the LJ clusters; in all cases, the species are liquidlike. For all cluster sizes, only small changes in $k_n^d(E, J)$ as a function of J are seen. The nature of these changes appear to be nonsystematic and probably due to mild sampling issues. The only deviation from this rule is represented by the case of LJ₁₉ at $E = -0.016$ hartree, for which $k_n^d(E, J)$ increases, roughly, by 20% for $J > 200$ a.u. Overall, the results shown in Fig. 2 support the previous observation on LJ₁₂₋₁₄ (Ref. 13) and Al₆ (Ref. 18) indicating a weak J -dependency of the dissociation rate. Bearing in mind the wide range of difference between the structure of the parent and daughter clusters explored in this work and Refs. 13 and 18, we interpret our numerical results (Fig. 2) as suggesting that it may be legitimate to neglect the dependency of $k_n^d(E, J)$ on J for atomic aggregates of similar size. As a direct consequence of this assumption, additionally the dependency of $k_n^d(E \rightarrow E', J \rightarrow J')$ on the angular momentum J' of the daughter cluster could be neglected while considering an evaporation cascade. This is easily understood: given the weak dependency on the angular momentum of the dissociation rate, there is no obligation to keep track of the amount of energy injected in the cluster rotational motion to describe a subsequent dissociation step. In this way, one is also relieved from the burden of estimating the probability of finding the

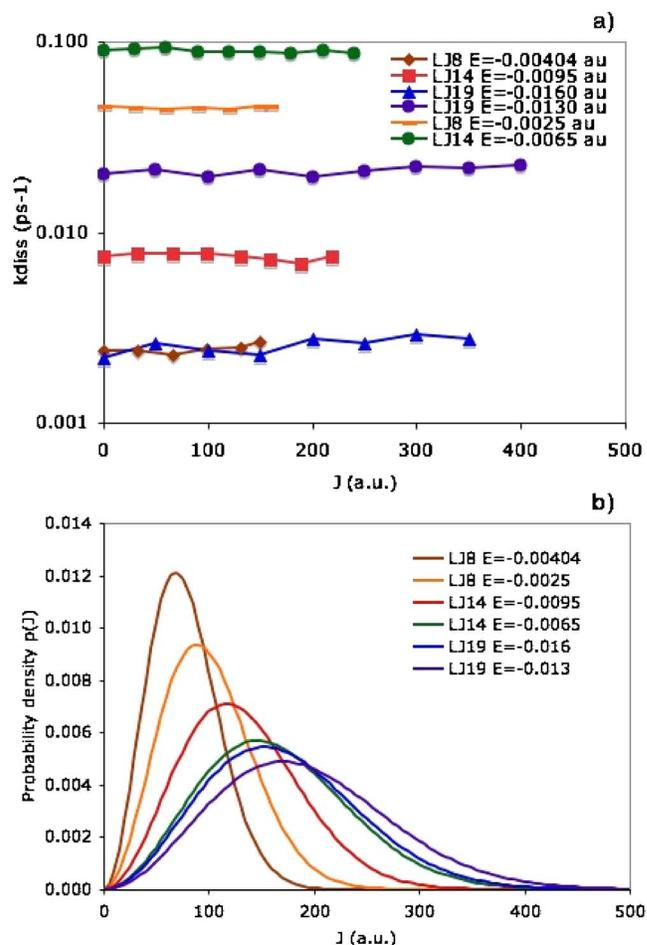


FIG. 2. (Color online) (a) $k_n^d(E, J)$ as a function of J (in units of \hbar) for LJ_{*n*} ($n=8, 14, 19$). Two selected values of E (potential plus rotational and vibrational kinetic energies, in atomic units) are shown per cluster size. E values were chosen to investigate the effect of medium and high energy content. J values were chosen to cover the range sampled during short preliminary simulations carried out with unconstrained J -sampling as described in the main text. Differences in $k_n^d(E, J)$ as a function of J are at most 20% in all cases. (b) A plot of the analytical form $p(J) = 4\sqrt{\alpha^3/\pi} J^2 \exp(-\alpha J^2)$, fitted to the sampled distribution of J , is shown for the six cases reported in panel a.

daughter cluster with total angular momentum J' given an initial total angular momentum J for the parent (see, however, Ref. 31 for an alternative approach that explicitly takes J' into account). This approximation is of course reasonable unless a substantial amount of rotational heating/cooling takes place during the dissociation processes, a possibility that, however, appears unlikely.¹⁵

In retrospective, the weak dependency of k_n^d on J highlighted by the MD results could have been easily foreseen from simple statistical consideration. Assuming equipartition of the internal energy between modes, one quickly reaches the conclusion that only a small fraction (roughly $3/[2(3n-6)+3]$) of the total energy would be into the rotational modes. This result, in turn, suggests that the vast majority of the energy needed during the dissociation process is made available by the vibrational modes, so that keeping track of the cluster rotational energy may generally not be of prime importance. In this way, a substantial simplification of the calculations and a reduction in the associated computational cost is introduced and we shall therefore assume in the rest

of this work that only a negligible dependency on the total angular momentum of the dissociation rates is present and focus only on the μ -ensemble.

B. Comparison between μ -vTST and MD dissociation rates

Bearing in mind the results discussed in the previous paragraphs, it appears therefore useful to benchmark the accuracy afforded by TST in predicting $k_n^d(E)$ for LJ clusters. Perhaps surprisingly, the only comparison between exact and statistical rates present in literature for these systems was carried out for PST on LJ₁₂₋₁₄,¹³ whereas no tests are available for the microcanonical version of TST provided by Eq. (6) to the best of our knowledge. In this situation, a more general test employing a set of atomic clusters featuring largely different structures appears as a worthwhile exercise as it could support more general conclusions.

To partially fill this gap, statistical and MD dissociation rate constants for LJ₈, LJ₁₄, and LJ₁₉ have been computed over a wider range of energies than explored in Sec. III A. MD simulations were run and analyzed with a protocol identical to the one used to investigate the J dependency of $k_n^d(E, J)$. As discussed in Sec. II, a microcanonical adaptation²⁵ of the procedure described in Ref. 27 was used to compute TST rates. This employs US to guide the configurational sampling close to the possible TS region and a discretization error-free estimator for the Dirac delta.²⁷ In the TST calculations, a variable number of US windows was used as a function of the cluster size (2 for LJ₈, 3 for LJ₁₄, and 5 for LJ₁₉). To reduce the likelihood of quasi-ergodic behavior for simulations at low energy, a microcanonical replica-exchange³² MMC approach was implemented according to the rules discussed in Ref. 33. In this approach, *all* MMC calculations needed to span the energy interval of interest for a given cluster are run concurrently, exchanging configurations between energetically close simulations with an exchange probability that conserves the microcanonical distribution at both energies. This allows configurations unlikely to be sampled by low energy simulations to “percolate down” from high energy ones, facilitating the sampling of region in configuration space separated by energy barriers. The set of energy values employed in the microcanonical MMC runs were chosen in order to obtain an exchange rate of, at least, 20%–30% between neighbor energy values during preliminary test simulations; 10⁶ configurations per energy were sampled during each US simulation. The value of $k_n^d(E)$ [Eq. (6)] was computed as a function of r_C over a grid of equispaced points separated by 1 bohr. Five to seven simulations were used to estimate these values obtaining a statistical accuracy of roughly 10%. The variational nature of TST rate constants was exploited selecting the location of the separatrix (r_C) over the chosen grid as the one that minimizes the value of $k_n^d(E)$. The simulation protocol employed for the TST calculations is fairly efficient and allows one to extend the range of energies substantially below the one accessible by MD thanks to its lower computational cost. In the energy range investigated, the clusters undergo a phase change from solidlike to liquidlike upon increasing the internal energy.

TABLE I. Monomer dissociation rates for LJ₈ as a function of the internal energy E computed using MD and TST simulations. The adiabatic dissociation energy for a monomer is 0.001 257 964 hartree for LJ₈. Statistical errors are of the order of 1% and 10% of the quoted results for MD and TST, respectively.

E (hartree)	$k_{\text{MD}}^d(E)$ (ps ⁻¹)	$k_{\text{TST}}^d(E)$ (ps ⁻¹)	$k_{\text{MD}}^d(E)/k_{\text{TST}}^d(E)$
-0.005	0.000 032	0.000 032	1.00
-0.004 75	0.000 13	0.000 16	0.81
-0.004 5	0.000 41	0.000 72	0.57
-0.004 25	0.001 1	0.002 2	0.50
-0.004 035	0.002 4	0.004 0	0.6
-0.003 5	0.008 1	0.013	0.62
-0.003	0.019	0.021	0.91
-0.002 5	0.045	0.033	1.37

The results of the MD and TST simulations are reported in Tables I–III and shown in Fig. 3. Tables I–III also report the recrossing factor $k_{\text{MD}}^d(E)/k_{\text{TST}}^d(E)$. From these data, one notices a good agreement between variational TST and MD rates, the two sets of data differing at most by a factor of 2 over the energy range accessible by MD simulations. As usual, TST deviates the most from MD at high energy, whereas low energy TST dissociation constants are off by less than 30%. To highlight the better computational performances of the TST based approach, in Table III we have also included rate constants computed in a range of E substantially lower than the one accessible by trajectory simulations for LJ₁₉. These additional results show that TST is, indeed, capable of providing an estimate for rates spanning roughly 20 orders of magnitude. As for the relative performances versus cluster size, the largest differences between TST and MD rates are seen for LJ₈ and LJ₁₉; we suspect this finding to be related to a less spherical structure for LJ₇ and LJ₁₈ than for LJ₁₃ and our choice of a spherical separatrix.

A more detailed analysis of the trajectory results indicated the presence of moderate nonstatistical effects for high energy species, with a slightly faster decay of $\ln[(N_0 - N_t)/N_0]$ at short time than at longer time (Fig. 4). To test for quasi-ergodic behavior, the slope of $\ln[(N_0 - N_t)/N_0]$ at $t=0$ was also computed. The latter was found to differ from

TABLE II. Monomer dissociation rates for LJ₁₄ as a function of the internal energy E computed using MD and TST simulations. The adiabatic dissociation energy for a monomer is 0.001 334 688 hartree. Statistical errors are of the order of 1% and 10% of the quoted results for MD and TST, respectively.

E (hartree)	$k_{\text{MD}}^d(E)$ (ps ⁻¹)	$k_{\text{TST}}^d(E)$ (ps ⁻¹)	$k_{\text{MD}}^d(E)/k_{\text{TST}}^d(E)$
-0.011		0.001 137 721	
-0.0105	0.0014	0.0021	0.67
-0.0100		0.0039	
-0.0095	0.0075	0.0062	1.23
-0.0085	0.013	0.015	0.87
-0.0080		0.023	
-0.0075	0.028	0.028	1.00
-0.0070		0.039	
-0.0065	0.051	0.046	1.1

TABLE III. Monomer dissociation rates for LJ₁₉ as a function of the internal energy E computed using MD and TST simulations. The adiabatic dissociation energy for a monomer is 0.002 324 973 hartree. To highlight the effectiveness of the TST approach, rate constant values at energies substantially below the ones accessible by MD simulations have also been included. Statistical errors are of the order of 1% and 10% of the quoted results for MD and TST, respectively.

E (hartree)	$k_{\text{MD}}^d(E)$ (ps ⁻¹)	$k_{\text{TST}}^d(E)$ (ps ⁻¹)	$k_{\text{MD}}^d(E)/k_{\text{TST}}^d(E)$
-0.024		7.7×10^{-24}	
-0.023		2.4×10^{-13}	
-0.022		4.6×10^{-9}	
-0.021		7.3×10^{-7}	
-0.02		0.000 022	
-0.019	0.000 094	0.000 12	0.78
-0.018	0.000 24	0.000 43	0.56
-0.017	0.001 1	0.001 7	0.64
-0.016	0.002 2	0.005 1	0.43
-0.015	0.005 9	0.010	0.59
-0.014	0.011	0.023	0.47
-0.013	0.020	0.039	0.51

the statistical rate constant by 10% at most, suggesting that the configuration space of all species is appropriately sampled by our MMC simulations and that the time dependence of $\ln[(N_0 - N_t)/N_0]$ is likely to derive from an “intrinsic non-Rice–Rampersberger–Kassel (RRK) behavior” as described by Bunker and Hase.³⁴ As far as obtaining an analytical representation for the behavior of k_n^d as a function of E , in the presence of intrinsic non-RRK behavior it should be possible to fit both the statistical and weakly nonstatistical regimes using the approach presented by Shalashilin and Thompson.³⁵ An analytical representation would, of course, facilitate the simulation of long evaporation cascades or droplet nucleation, a long term interest of ours.

Apart from exploring the possibility of nonstatistical behavior during cluster dissociation, the possible impact of anharmonicity on $k_n^d(E)$ was assessed by fitting low energy TST rates for all clusters with the RRK expression $\log[k_n^d(E)]$

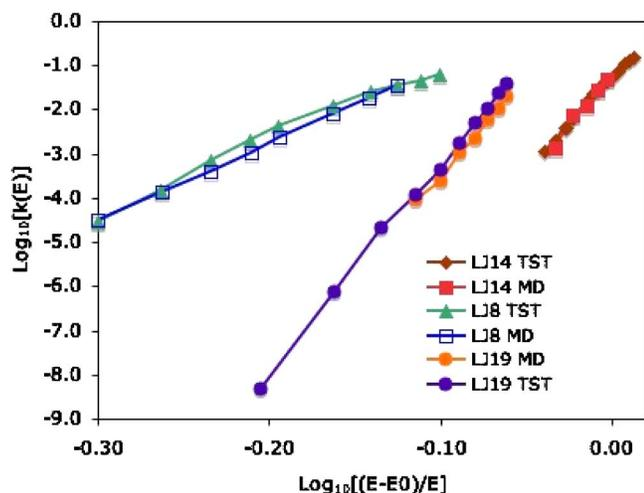


FIG. 3. (Color online) Behavior of $\log_{10}[k_n^d(E)]$ (ps⁻¹) as a function of $\log_{10}[(E - E_0)/E]$ for $n=8, 14$, and 19 . The data for LJ₁₄ have been shifted by 0.05 units of $\log[(E - E_0)/E]$ to the right in order to unclutter the plot.

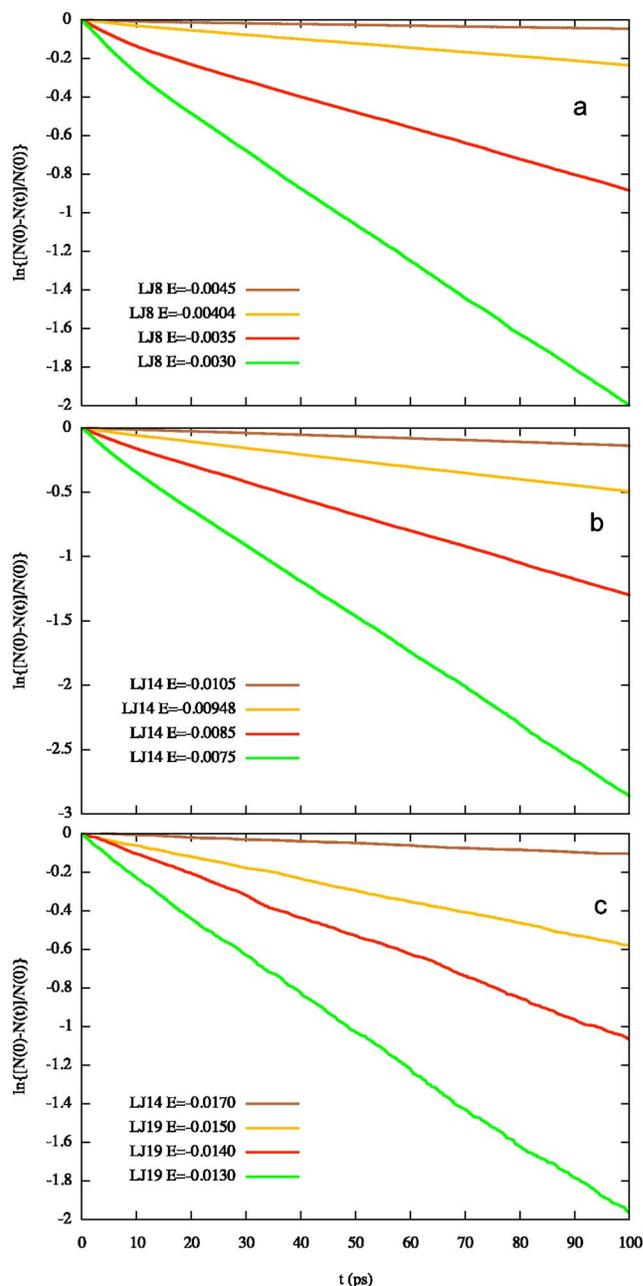


FIG. 4. (Color online) Behavior of $\ln[(N_0 - N_t)/N_0]$ vs time for selected values of the internal energy (in a.u.). (a) LJ₈; (b) LJ₁₄; (c) LJ₁₉.

$= \log(\nu) + (s-1)\log[(E - E_0)/E]$. Here, E is the internal energy of the cluster and E_0 is its evaporation energy (i.e., the energy necessary to detach a monomer from the global minimum of LJ _{n} producing the global minimum of LJ _{$n-1$}). Overall, the RRK expression was found to performed quite well, even though the fitting process produced larger s values than suggested by counting the vibrational degrees of freedom ($s_{\text{RRK}} = 3 \times n - 6$) for LJ₈ and LJ₁₄. Specifically, s was found to be 22, 44, and 50 for $n=8, 14$, and 19 , respectively. According to Song and Hase,³⁶ an s value larger than the number of modes is likely to be due to anharmonic effects, which allow the sum of states for the TS ($N^\ddagger(E)$) to grow more rapidly than the reactant density of states ($\rho(E)$). This seems to be the case for both LJ₈ and LJ₁₄ that are liquidlike in the range of energies used to extract s . Differently, LJ₁₉ is solid-

like in the range of E employed in the fitting procedure and the obtained s value, only slightly lower than the theoretical s_{RRK} , seems to suggest that the cluster is behaving in reasonable accord with the harmonic approximation used to derive the RRK rate expression. An additional deviation from the classical RRK behavior might be present in barrierless dissociations due to a contraction of the TS distance upon increasing the internal energy. This contraction may affect both the effective value of the dissociation energy and the absolute value of ν (for harmonic modes this term is given by $\nu = \prod_{i=1}^s \nu_i / \prod_{i=1}^{s-1} \nu_i^\ddagger$,³⁰ where ν_i and ν_i^\ddagger are the harmonic frequencies of the reactant and TS, respectively). However, we found only small changes (1 bohr) in the locations of the TS as a function of E , suggesting a minor role for this effect.

To conclude this section, it appears necessary to comment on the total cost of both MD and statistical TST simulations, providing evidence for the better efficiency and reduced computational effort suggested earlier for MMC-TST calculations. To do so, let us focus on the largest and most demanding cluster studied, namely, LJ₁₉. For this, obtaining low energy MD dissociation rates required a minimum of 2500 trajectories and roughly 55 min per energy on an Intel 3.0 GHz processor. In those conditions, we found that only a small fraction (e.g., 60 over 2500) of trajectories are reactive and that the total computational time decreases by up to a factor of 3 due to faster trajectory dissociation at higher energy. To estimate TST rates, five US windows were used to force the MMC simulation to visit the relevant range of r_{IRC} (16–40 bohr), each of which sampled 10^6 configurations at 12 different energies and required roughly 20 min. Six additional simulations of similar length were successively employed to estimate $\langle \delta(r_{\text{IRC}} - r_C) \rangle$, with a total cost of roughly 18 min per energy. As a consequence, TST allows a threefold decrease in computational time at the lowest energy still amenable to MD simulations.

C. KER distributions

From the results discussed in Sec. III B, we conclude that the version of TST given by Eq. (6) may indeed be capable of providing accurate dissociation rate constants for LJ_{*n*} over a wide range of energies and a substantial saving in computer time for processes at low energy. It would seem therefore possible to rely on MD simulations only for the most difficult cases or at high values of E .

In our view, there is an additional and more compelling reason to employ TST in modeling the dissociation of atomic and molecular clusters, a reason that has been partially introduced in the work by Calvo and Parneix.²⁰ As discussed in Sec. I, modeling a cluster dissociation cascade by means of a set of MEs necessitates use of either $P_{ir}(E, \epsilon_{ir})$ (the distribution of E_{ir} as a function of E and J) or $P_i(E, \epsilon_i)$ (the distribution of E_i as a function of E if the J -dependency is neglected). Unfortunately, obtaining a precise estimate for these distributions with MD is more demanding than the calculation of $k_n^d(E)$. For instance, we found that a minimum of 10 000 *dissociated* trajectories were needed to obtain a reasonably precise $P_{ir}(E, \epsilon_{ir})$ for LJ₈. From these data and the small fraction of low energy dissociation events witnessed

for LJ₁₉ (roughly 2.5%), it is possible to estimate that at least 153 h would be needed to obtain a low energy KER distribution for LJ₁₉.

The difficulty related to the large number of dissociated trajectories needed for the construction of $P_{ir}(E, \epsilon_{ir})$ could, in principle, be circumvented using TST. In fact, Calvo and Parneix¹⁵ already showed that accurate KER distributions can be obtained using PST at a small fraction of the computational cost required by MD (Ref. 15) provided that $\Omega(E)$ and the correct integration boundaries in energy and momentum space are available. As mentioned previously, Eq. (8) circumvents the necessity for an accurate estimate of $\Omega(E)$ and it is expected to feature a similarly reduced computational cost. However, the performance of Eq. (8) in predicting $P_{ir}(E, \epsilon_{ir})$ need to be properly assessed, the results of this task being described in the following paragraphs.

To produce a comparison for $P_{ir}^{\text{TST}}(E, \epsilon_{ir})$ (Eq. (8)), at least 10 000 dissociated MD trajectories have been collected for each cluster size and value of internal energy investigated. Trajectory simulations have been carried out following protocols discussed in Secs. III A and III B. More specifically, trajectories were dubbed as dissociated at $r_{\text{IRC}} = 4\sigma$ and analyzed to extract both E_i and E_r with the scheme proposed in Sec. II for the analysis of the TST simulations. Histograms for $P_{ir}^{\text{TST}}(E, \epsilon_{ir})$ were obtained collecting samples composed of 10^4 independent configurations distributed accordingly to the μ -TS ensemble by means of MMC simulations. In the latter, Jacobi coordinates were used instead of the Cartesian ones to maintain the dissociating atom on the separatrix. For each configuration \mathbf{q} extracted from the MMC runs, 20 independent momentum samples were generated as suggested earlier, producing a total of 2×10^5 independent momentum samples for energy and cluster size.

Figure 5 shows the KER distributions for the three cluster sizes and selected values of the internal energy. Overall, the results presented in Fig. 5 indicate a good agreement between MD and TST distributions, especially at low internal energy. At higher internal energies, the agreement slightly deteriorates for low values of ϵ_{ir} , whereas the behavior at high ϵ_{ir} is reasonably well reproduced (panels a and b). More specifically, the TST distributions suggest a higher probability for low ϵ_{ir} values than the MD counterparts. A similar behavior (not shown) was also found for the distribution of E_i .

At the moment, we find it difficult to completely rationalize the difference between MD and TST results. This may be due, for instance, to nonstatistical effects, i.e., to nonstatistical energy distributions in the products, which may lead to a more substantial accumulation of energy either along the reaction coordinate or in the rotational motion of the fragment cluster. Another possible source of difference comes from the fact that different separatrix locations are used in MD and TST simulations, the optimized separatrix radius r_C in TST always being shorter than the fixed distance $r_C = 4\sigma$ used for MD trajectories. Because a phase space point is implicitly labeled as “reactive” in Eq. (7) based only on a positive value of the projection of its velocity along the reaction coordinate, some residual interaction between the two fragments may still be present due to the shorter r_C

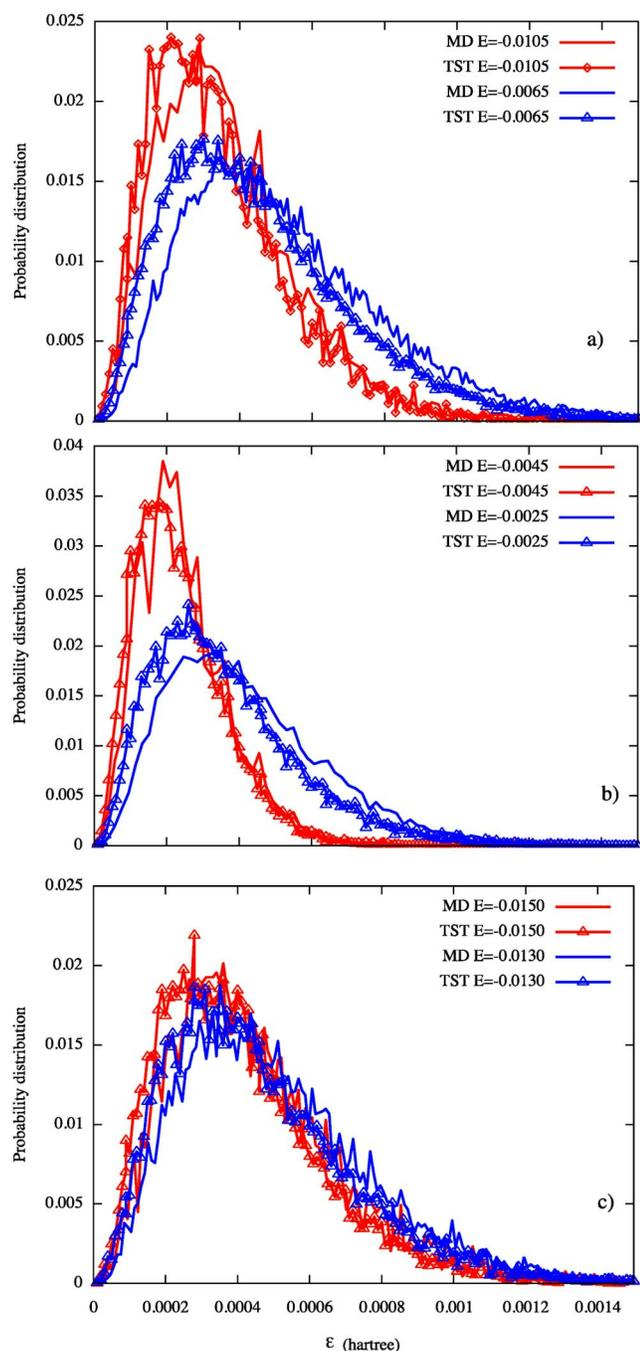


FIG. 5. (Color online) MD and TST KER distribution for LJ_n at different values of E . (a) $n=14$; (b) $n=8$; (c) $n=19$. The distributions have been normalized so that $\int P(E, \epsilon_{ir}) d\epsilon_{ir} = 1$. Energy in hartree.

distance used in TST. As a consequence of this, not all the phase space points dubbed as reactive in TST should be considered as such, and the ones with only a small amount of kinetic energy injected along r_{IRC} may actually be “trapped.” Excluding the contribution of such points should lead to a decrease in the probability of emitting a monomer at low ϵ_{ir} . Needless to say, both nonstatistical effects and the limitation intrinsic in the choice of a geometric separatrix may share a role in inducing the discrepancy between KER distributions at low ϵ_{ir} , an issue that would be the focus of an investigation in the near future.

IV. CONCLUSIONS

This work reports an investigation exploring the possibility of theoretical and computational simplifications that could be introduced in studying the quantitative details of dissociating atomic clusters. The underlying motivation behind this study is the desire of extending DNT to the microcanonical ensemble (or the J -resolved microcanonical ensemble), the latter being a more natural framework to deal with gas phase activated processes such as collision-induced dissociation.

The first simplification comes from noticing that $k_n^d(E, J)$ is substantially independent of J , the total angular momentum of the activated aggregate, for the range of cluster sizes and energies explored in this work. As a net consequence of this, one would therefore be allowed to focus only on the energy dependency of k_n^d with a substantial reduction in both the complexity and cost of the calculations. However, it is important to stress that the reason for introducing this simplification is only related to the total cost of computing dissociation rates and not to an intrinsic limitation of TST in dealing with nonzero angular momentum. In fact, it would be straightforward to extend it using the procedure suggested in Ref. 31.

When modeling parallel dissociation/condensation processes, the weak sensitivity of $k_n^d(E, J)$ with respect to J may allow one to introduce another simplification in the ME set, namely the possibility of neglecting the dependency on J of the condensation rate constant $k_{n-1}^c(E' \rightarrow E, J' L' \rightarrow J)$, L' indicating the orbital angular momentum of the colliding system. Similarly to that discussed previously, this simplification would rely on the fact that the dissociation lifetime of M_n only weakly depends on J , but it would be fully justified only if k_{n-1}^c was also found to be largely independent of J' , an issue currently under investigation in our laboratory.

As for the dependency of $k_{n-1}^c(E' \rightarrow E, J' L' \rightarrow J)$ on L' , indirect evidence for a simple behavior of k^c with respect to L' was provided by Napari *et al.*,³⁷ who carried out MD simulations to study the monomer capture probability by cold LJ clusters as a function of the collision parameter b . The capture probability (and the lifetime τ of the formed cluster) was found to be practically insensitive to b , hence to L' , provided b was within the cluster radius. At larger collision parameters, the capture probability becomes almost negligible suggesting the possibility of modeling the condensation process as a function of L' using a steplike function for the capture probability. Notice, however, that Georgievskii and Klippenstein³⁸ reported improvements in the accuracy of long range TST when the full μJ -vTST version is used. Needless to say, a more accurate investigation of this issue for atomic clusters would be worthwhile but it is outside the scope of this work.

Evidence has been also provided for a good performance of TST with respect to MD in predicting the dissociation rate constant as a function of the aggregate internal energy E . Bearing in mind that usually TST performs rather well at low energy, i.e., when MD becomes inefficient, this finding suggests that statistical $k_n^d(E)$'s obtained with Eq. (6) could be used at all but the highest values of internal energy with a

substantial saving in computational time. Importantly, the version of TST used in this work [see Eq. (6)] lends itself to be merged with a microcanonical extension of replica exchange algorithm,³² thus improving the exploration of the configuration space, and fully accounts for the anharmonic behavior of LJ_n . As previously shown by Peslherbe and Hase¹⁸ for PTS, the correct treatment of anharmonicity is an indispensable ingredient for an accurate prediction of dissociation rates for fluxional species.

The knowledge of $k_n^d(E)$ over a wide range of energies would, in principle, allow one to also obtain $k_n^d(T)$ by convolving the NVE reaction rates with the normalized Boltzmann distribution $P_n^B(T, E)dE = \Omega(E)e^{-E/k_B T}dE / \int \Omega(E)e^{-E/k_B T}dE$ for LJ_n at the chosen temperature T . According to this prescription, one also needs to know $\Omega(E)$, the system density of states, in order to obtain $k_n^d(T)$. Unfortunately, the accurate calculation of $\Omega(E)$ is far from trivial (see e.g., Ref. 20 for a discussion), explicitly avoided by the method described in Sec. II, and it is therefore considered outside the scope of this work. Besides, we suspect that the direct calculation of $k_n^d(T)$ using, for instance, the approach described in Ref. 27 would be as efficient, if not more, than obtaining $\Omega(E)$ and, subsequently, computing the convolution integral.

Finally, the performance of a TST-based approach [Eq. (8)] to predict KER distributions has been tested against MD results and shown to provide quantitative accuracy at low internal energies. At higher energies, the agreement slightly deteriorates, probably due to nonstatistical behavior or to the different method used to label a phase space point as reactive. Nevertheless, our approach appears to provide, overall, a robust and computationally efficient tool for the calculation of this important quantity.

Armed with the simplifications discussed above, TST could therefore become a powerful tool to study the atomistic details of cluster dissociation cascades. Needless to say, several issues still need to be addressed before it becomes of general applicability. In this respect, it is important to point out that better choices for the separatrix (e.g., nonspherical or momentum dependent) may further improve its accuracy and that further algorithmic development is likely to reduce the computational cost with respect to trajectory simulations even more. Work in these directions is currently carried out in our laboratory.

With the long term goal of simulating homogeneous vapor-liquid condensation, one should also be concerned with the performance of TST in predicting the capture of a monomer by an already formed aggregate and the subsequent dissociation or de-energization process that may be induced by a postcapture collision with another body. The latter processes may, in principle, be modeled also in the TST framework³⁹ provided that the lifetime of the energized cluster is long enough to allow for intrasystem energy redistribution. Evidence for well separated time scales between energy redistribution and dissociation has been provided by Napari and Vehkamäki,⁴⁰ who highlighted the short time required for energy redistribution (maximum 30 ps) and the small role played by unrelaxed clusters. Given the fact that

the $k_n^d(E)$ values reported in this work suggest a cluster lifetime at least an order of magnitude longer, it would be interesting to explore the overall accuracy of a two step TST approach to the condensation/dissociation process.

ACKNOWLEDGMENTS

The author wishes to acknowledge Emanuele Curotto, Fausto Cargnoni, and Gabriele Morosi for the help and many suggestions on how to clarify this manuscript, and Samuel L. Stone for a careful read.

- ¹J. Wedekind and D. Reguera, *J. Chem. Phys.* **127**, 154516 (2007).
- ²H. Matsubara, T. Koishi, T. Ebisuzaki, and K. Yasuoka, *J. Chem. Phys.* **127**, 214507 (2007).
- ³S. Toxvaerd, *J. Chem. Phys.* **115**, 8913 (2001).
- ⁴P. Schaaf, B. Senger, J.-C. Voegel, R. K. Bowles, and H. Reiss, *J. Chem. Phys.* **114**, 8091 (2001).
- ⁵K. K. Tanaka, K. Kawamura, H. Tanaka, and K. Nakazawa, *J. Chem. Phys.* **122**, 184514 (2005).
- ⁶P. R. ten Wolde and D. Frenkel, *J. Chem. Phys.* **109**, 9901 (1998).
- ⁷J. Merikanto, E. Zapadinsky, A. Lauri, and H. Vehkamäki, *Phys. Rev. Lett.* **98**, 145702 (2007).
- ⁸G. K. Schenter, S. M. Kathmann, and B. C. Garrett, *J. Chem. Phys.* **110**, 7951 (1999).
- ⁹P. Schaaf, B. Senger, J.-C. Voegel, R. K. Bowles, and H. Reiss, *J. Chem. Phys.* **114**, 8091 (2001).
- ¹⁰J. C. Barrett, *J. Chem. Phys.* **126**, 074312 (2007).
- ¹¹L. D. Crosby, S. M. Kathmann and T. L. Windus, *J. Comput. Chem.*, DOI:10.1002/jcc.21098 (2008).
- ¹²J. W. Brady, J. D. Doll, and D. L. Thompson, *J. Chem. Phys.* **74**, 1024 (1981).
- ¹³S. Weerasinghe and F. G. Amar, *J. Chem. Phys.* **98**, 4967 (1993).
- ¹⁴S. A. Harris and I. J. Ford, *J. Chem. Phys.* **118**, 9216 (2003).
- ¹⁵F. Calvo and P. Parneix, *J. Chem. Phys.* **119**, 256 (2003).
- ¹⁶P. Pechukas and J. C. Light, *J. Chem. Phys.* **42**, 3281 (1965).
- ¹⁷W. J. Chesnavich and M. T. Bowers, *J. Chem. Phys.* **66**, 2306 (1977).
- ¹⁸G. H. Peslherbe and W. L. Hase, *J. Chem. Phys.* **105**, 7432 (1996).
- ¹⁹G. K. Schenter, S. M. Kathmann, and B. C. Garrett, *J. Chem. Phys.* **116**, 4275 (2002).
- ²⁰F. Calvo and P. Parneix, *J. Chem. Phys.* **126**, 034309 (2007).
- ²¹F. H. Mies, *J. Chem. Phys.* **51**, 798 (1969).
- ²²H. W. Schranz, S. Nordholm, and B. C. Freasier, *Chem. Phys.* **108**, 69 (1986).
- ²³H. W. Schranz, S. Nordholm, and G. Nyman, *J. Chem. Phys.* **94**, 1847 (1991).
- ²⁴H. W. Schranz, L. M. Raff, and D. L. Thompson, *J. Chem. Phys.* **94**, 4219 (1991).
- ²⁵M. Mella, *J. Chem. Phys.* **124**, 104302 (2006).
- ²⁶G. M. Torrie and J. P. Valleau, *J. Comput. Phys.* **23**, 187 (1977).
- ²⁷M. Mella, *J. Chem. Phys.* **128**, 244515 (2008).
- ²⁸E. K. Grimmelmann, J. C. Tully, and E. Helfand, *J. Chem. Phys.* **74**, 5300 (1981).
- ²⁹E. S. Severin, B. C. Freasier, N. D. Hammer, D. L. Jolly, and S. Nordholm, *Chem. Phys. Lett.* **57**, 117 (1978).
- ³⁰T. Baer and W. L. Hase, *Unimolecular Reaction Dynamics* (Oxford University Press, Oxford, 1996).
- ³¹R. S. Dumont and S. Jain, *J. Chem. Phys.* **103**, 6151 (1995).
- ³²R. H. Swendsen and J.-S. Wang, *Phys. Rev. Lett.* **57**, 2607 (1986).
- ³³E. Curotto and D. L. Freeman, and J. D. Doll, *J. Chem. Phys.* **109**, 1643 (1998).
- ³⁴D. L. Bunker and W. L. Hase, *J. Chem. Phys.* **59**, 4621 (1973).
- ³⁵D. V. Shalashilin and D. L. Thompson, *J. Chem. Phys.* **105**, 1833 (1996).
- ³⁶K. Song and W. L. Hase, *J. Chem. Phys.* **110**, 6198 (1999).
- ³⁷I. Napari, H. Vehkamäki, and K. Laasonen, *J. Chem. Phys.* **120**, 165 (2004).
- ³⁸Y. Georgievskii and S. J. Klippenstein, *J. Chem. Phys.* **122**, 194103 (2005).
- ³⁹J. C. Keck, *J. Chem. Phys.* **32**, 1035 (1960).
- ⁴⁰I. Napari and H. Vehkamäki, *J. Chem. Phys.* **124**, 024303 (2006).